# Effects of $^3$He impurities on the mass decoupling of $^4$He films

Kenji Ishibashi,[1] Jo Hiraide,[1] Junko Taniguchi,[1,*] Tomoki Minoguchi,[2] and Masaru Suzuki[2,†]
[1]*Department of Engineering Science, University of Electro-Communications, Chofu, Tokyo 182-8585, Japan*
[2]*Institute of Physics, University of Tokyo, Meguro-ku, Tokyo 153-8902, Japan*

(Received 14 January 2020; revised 27 August 2020; accepted 31 August 2020; published 14 September 2020)

We performed quartz crystal microbalance experiments using a 5-MHz AT-cut crystal for superfluid $^4$He films on exfoliated graphite (Grafoil) containing up to 0.40 atom/nm$^2$ $^3$He. We found that the mass decoupling of $^4$He solid layers from the oscillating substrate is considerably sensitive, even with small amounts of $^3$He. For a $^4$He film of 29.3 atoms/nm$^2$, we observed a small drop in resonant frequency at a $T_3$ of ∼0.4 K for a low oscillation amplitude, which is attributed to the sticking of $^3$He atoms at the $^4$He solid layer. For higher amplitudes, the $^4$He solid layer shows a reentrant mass decoupling at $T_R$ close to $T_3$. This decoupling can be explained by the suppression of the superfluid counterflow owing to the adsorption of the $^3$He atoms on edge dislocations. As the $^4$He areal density increases, $T_R$ shifts to a lower temperature and disappears around the $^4$He film of 39.0 atoms/nm$^2$.

DOI: 10.1103/PhysRevB.102.104104

## I. INTRODUCTION

It is well established that the surface of graphite is atomically flat and the helium film on graphite grows layer by layer to a film that is more than five atoms thick [1,2]. Because of the quantum nature of helium and its ideal two-dimensional system, helium film on graphite has attracted the attention of many researchers as a model system, with its adsorbed structure [1,3,4], magnetism [5,6], and superfluidity [2,7] all having been extensively studied both experimentally and theoretically.

Recently, the nanofriction, or mass decoupling from oscillation, of films has been widely discussed [8]. Several metal substrate films exhibit partial mass decoupling [9]. Studies have also been conducted on films during the pinning-depinning transition in which a critical driving force is applied to an oscillating substrate [10].

In response to the study on nanofriction, we began to study the mass decoupling of helium films on graphite using a quartz crystal microbalance (QCM) technique. To date, we have reported the following observations [11–14]:

(a) During high oscillation amplitudes, the solid layers above two-atom-thick films were found to undergo partial mass decoupling below a certain temperature $T_S$.

(b) This decoupling resulted in a low-frictional metastable state when overlaid with normal fluid. After a reduction in amplitude, the solid layer remained in a low-frictional state within a finite lifetime.

(c) For a superfluid overlayer, the mass decoupling was found to vanish rapidly at $T_D$ below $T_S$.

(d) The mass decoupling behavior was similar for the $^3$He films up to five atoms thick without an abrupt suppression due to the superfluid.

The film inhomogeneity plays an important role in this decoupling process. We proposed the following scenario [13], with the knowledge that the edge dislocation motion in the solid layer is responsible for mass transport: mass decoupling occurs when the edge dislocation overcomes the potential barriers (i.e., Peierls potential). This explains the external force threshold for mass decoupling and the low-frictional metastable state. The sudden disappearance of this feature below $T_D$ can be explained by the cancellation of mass transport owing to the counterflow of the superfluid overlayer.

As the mass decoupling of helium films has shown various behaviors, in this study, we limit ourselves to examining the $^3$He impurity effects of the $^4$He films on exfoliated graphite (Grafoil) under a superfluid overlayer using a MHz-range AT-cut crystal. After a brief explanation of the experimental procedure in Sec. II, we present the $^3$He areal density dependence in Sec. III A for a four-atom-thick film at various oscillation amplitudes. By adding a small amount of $^3$He to the film, we found that the mass decoupling reappears at a certain temperature ($T_R$) below $T_D$, especially at higher amplitudes. In Sec. III B, we reveal the $^4$He areal density dependence on $^3$He. Here, $T_R$ was found to decrease with increasing $^4$He areal density before disappearing. In addition to these observations, we discuss a possible mechanism for the reentrant mass decoupling at $T_R$.

## II. EXPERIMENTAL PROCEDURE

The QCM technique was used with an AT-cut crystal to measure the mass decoupling of the films. For this QCM technique, the mass coupled to the oscillating substrate is obtained from the change in resonant frequency, $\Delta f$, as

$$\frac{\Delta f}{f} = -\frac{m}{M}, \tag{1}$$

where $m$ is the coupled mass of the film, $M$ is the oscillating mass of the crystal, and $f$ is the resonant frequency [15].

*tany@phys.uec.ac.jp
†suzuki@phys.uec.ac.jp

 

When the film is decoupled from the oscillation, the coupled mass decreases with an increase in resonant frequency.

For these experiments, the resonator consisted of a 5.0-MHz AT-cut crystal. The crystal was commercially sourced, with no additional treatment applied to the Ag electrode. The Grafoil was first baked in a vacuum at 900°C for 3 h, with a 300-nm Ag film subsequently deposited onto its surface. The AT-cut crystal and Ag-plated Grafoil were pressed together before heating in a vacuum at 350°C for 2 h. The Grafoil was then bonded to both sides of the Ag electrode. After bonding, any excess Grafoil was removed to increase the $Q$ value of the crystal. For good thermal contact, the crystal was fixed to the metal holder using an electrically conductive adhesive. After this, the $Q$ value was better than $10^4$ when the areal density of Grafoil was 7.30 g/m$^2$. Following the heat treatment at 130°C for 5 h under a pressure of $2 \times 10^{-6}$ Pa, the crystal was mounted onto a sample cell. Here, the mass loading for the $^4$He layers was found to be 3.8 Hz $\cdot$ atoms$^{-1}$ $\cdot$ nm$^2$.

A transmission circuit was used to measure the resonant frequency. In this circuit, the crystal was placed directly across a series of coaxial lines connected to a 50-Ω continuous-wave signal generator and radio-frequency lock-in amplifier. The frequency of the signal generator was controlled with the resonant frequency locked to maintain the in-phase output at 0. The quadrature output at this frequency is the amplitude of resonance.

In these experiments, the $^3$He areal density only reached 0.4 atom/nm$^2$, which corresponds to an areal density of 5% for one atomic layer of $^4$He.

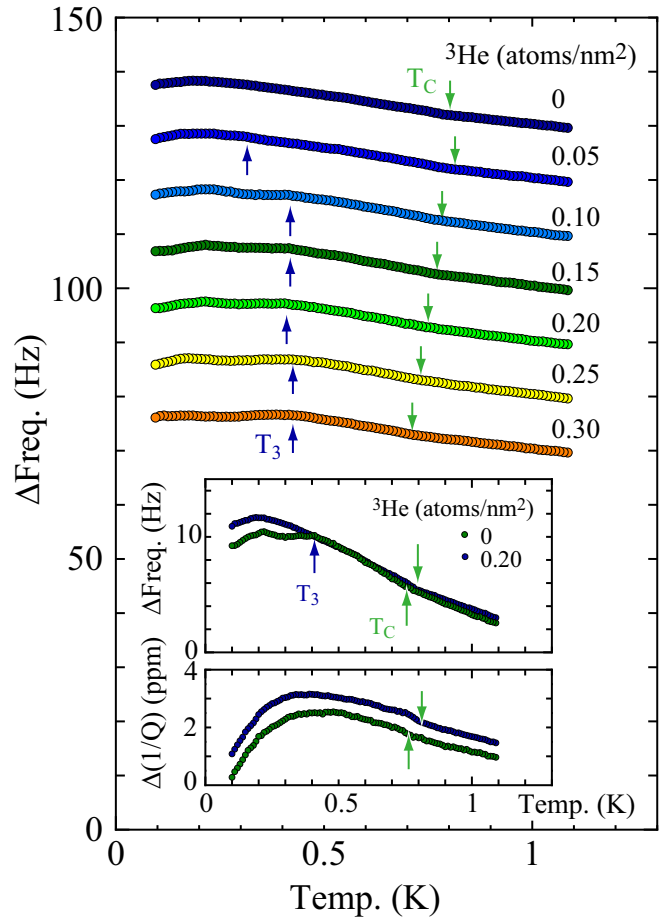


FIG. 1. Variation in resonant frequency of a 29.3 atoms/nm$^2$ $^4$He film at a 0.018-nm amplitude for various $^3$He areal densities. Arrows indicate the superfluid onset temperature $T_C$ and the $^3$He adsorption temperature $T_3$. Data are shifted vertically. Inset: Comparison of the resonant frequency and $Q$ value between the pure $^4$He film and the $^4$He film containing 0.20 atom/nm$^2$ $^3$He (run A).

## III. RESULTS AND DISCUSSION

### A. $^3$He areal density dependence

For the temperature sweep experiments, we used $^4$He films approximately four atoms thick under various oscillation amplitudes through a change in the $^3$He areal density (run A).

Figure 1 shows the variation in resonant frequency for $^4$He films with 29.3 atoms/nm$^2$ and various $^3$He areal densities. It can be seen that the film overlayers undergo superfluidity at low temperatures. All data points were taken during the cooling process, with the oscillation amplitude fixed at 0.018 nm. Here, the onset of superfluidity for the pure $^4$He film was clearly observed at a $T_C$ of 0.80 K, although it is difficult to observe in Fig. 1. As the $^3$He areal density increased, $T_C$ was found to decrease gradually. For the $^4$He film containing 0.30 atom/nm$^2$ $^3$He, $T_C$ is seen to shift down to 0.75 K. With additional doses of $^3$He, a small drop in the resonant frequency was found to occur at $T_3$ below $T_C$. This drop became more evident as the $^3$He areal density increased. In contrast, $T_3$ does not appear to depend too strongly on the $^3$He areal density, particularly above 0.1 atom/nm$^2$.

In the inset in Fig. 1, we compare the variation in resonant frequency and $Q$ value between the pure $^4$He film and the $^4$He film containing 0.20 atom/nm$^2$ $^3$He. For the pure $^4$He film, the onset of superfluidity occurred at a $T_C$ of 0.80 K, in addition to a small increase in $\Delta(1/Q)$. After adding 0.20 atom/nm$^2$ $^3$He, $T_C$ was found to shift slightly downward to 0.76 K. The resonant frequency decreased at a $T_3$ of 0.41 K from the extrapolated curve at higher temperatures. The differences are shown to increase gradually, particularly at the lowest attainable temperature of 0.1 K, where it then becomes 1.5 Hz. Unfortunately, an anomaly in $\Delta(1/Q)$ was not accurately observed at $T_3$.

It is natural that the observed drop below $T_3$ is connected to the addition in $^3$He. The mass loading of $^3$He is estimated to be 2.9 Hz $\cdot$ atoms$^{-1}$ $\cdot$ nm$^2$ based on that of $^4$He. The drop of 1.5 Hz at a low temperature corresponds to 0.5 atom/nm$^2$ loading in $^3$He. This value is approximately double that of the $^3$He dopant. We therefore concluded that the drop below $T_3$ is caused by the sticking behavior of the $^3$He atoms on the $^4$He solid layer, as well as through the prevention of $^4$He atom decoupling. Moreover, we found that $T_3$ is independent of the $^3$He areal density above 0.1 atom/nm$^2$, suggesting that the number of atomic adsorption sites for $^3$He is approximately 0.1 nm$^{-2}$.

It is established that for $^3$He - $^4$He solids, $^3$He atoms are trapped on dislocation cores with an adsorption potential of 0.7 K [16]. One potential adsorption site on the $^4$He solid layers is also from the edge dislocations. Because of the

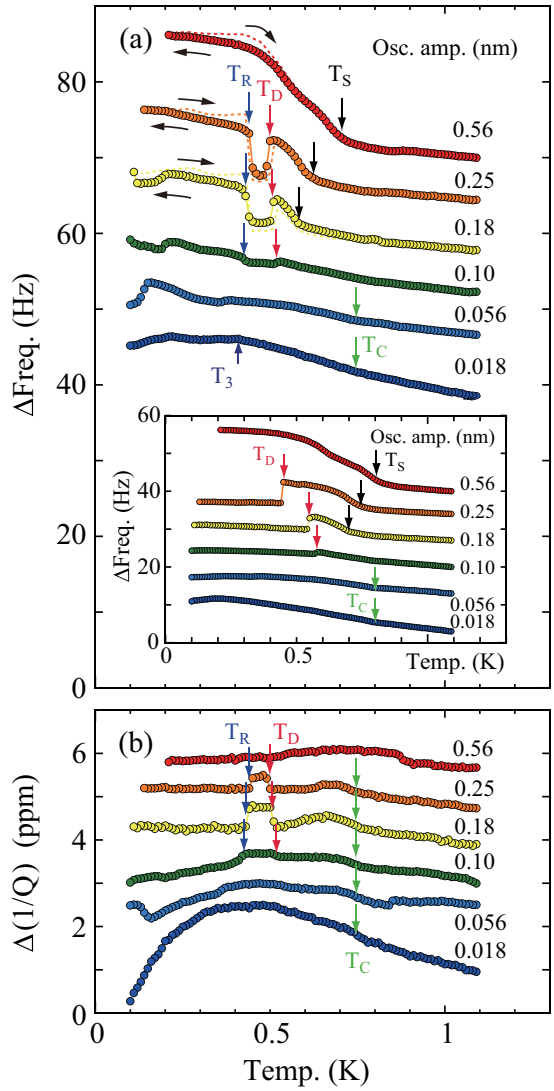


FIG. 2. (a) Variation in resonant frequency of a 29.3 atoms/nm$^2$ $^4$He film containing 0.20 atom/nm$^2$ $^3$He for various oscillation amplitudes (run A). Arrows indicate the decoupling temperature $T_S$, the sticking temperature $T_D$, and the reentrant decoupling temperature $T_R$. Data are shifted vertically. Inset: Variation in resonant frequency of pure $^4$He film at 29.3 atoms/nm$^2$ during the cooling process. (b) Variation in $\Delta(1/Q)$ for various oscillation amplitudes.

adsorption potential of graphite, the first atomic layer is approximately 20% denser than the second [1]. From the density difference between the solid layers, it is natural to assume that the second atomic layer consists of commensurate domains separated by domain walls. With domain walls almost characteristic of edge dislocations [13], we refer to these as edge dislocations.

Here, it should be noted that the thickness of the fluid overlayer is at most only one atomic layer, and thus, $^3$He atoms may not be floated on the free surface, in contrast to bulk liquid $^4$He [17].

Figure 2(a) shows the amplitude dependence of the $^4$He film containing 0.20 atom/nm$^2$ $^3$He. The data points denoted by filled circles were taken during the cooling process, whereas those denoted by short-dashed lines were from the warming process. As shown in Fig. 1, for an amplitude of 0.018 nm, the onset of superfluidity and a drop in frequency were observed at a $T_C$ of 0.76 K and a $T_3$ of 0.41 K. As the amplitude increased to 0.056 nm, no drop in frequency at 0.41 K occurred.

For amplitudes of 0.18, 0.25, and 0.56 nm, the resonant frequency is shown to increase clearly at $T_S$, before terminating abruptly at $T_D$. As shown in the inset in Fig. 1, this behavior is also observed for the pure $^4$He film and attributed to the decoupling and sticking behavior of the $^4$He solid layer.

Through the addition of small amounts of $^3$He, we see a new phenomenon appear. Below $T_D$, the resonant frequency is shown to increase at a certain temperature, $T_R$, suggesting that the $^4$He solid layer undergoes decoupling. We found the reentrant mass decoupling temperature, $T_R$, close to $T_3$, i.e., the temperature at which the $^3$He atoms are trapped at an adsorption site on the $^4$He solid layer. For an amplitude of 0.56 nm, $T_D$ and $T_R$ disappear, causing the $^4$He solid layer to decouple at a lower temperature.

Figure 2(b) shows the variation in $\Delta(1/Q)$. As shown in Fig. 1, for an amplitude of 0.018 nm, $\Delta(1/Q)$ increased slightly below a $T_C$ of 0.76 K. As the amplitude increased to 0.25 nm, the slight increase in $\Delta(1/Q)$ remained. This indicates that the heating of QCM does not significantly affect the observed results.

To determine the $^3$He areal density dependence of $T_S$, $T_D$, and $T_R$, we performed a series of temperature sweep experiments at an amplitude of 0.25 nm. Figure 3 shows the resulting variations in resonant frequency. All data points were taken during the warming process. When 0.05 atom/nm$^2$ $^3$He was added, the decoupling and sticking behaviors were found to drastically change compared with those of the pure $^4$He film. The $T_S$ also decreased to 0.69 K in comparison with that of the pure $^4$He film at 0.74 K, whereas the $T_D$ did not change significantly at 0.50 K. As the temperature decreased, the resonant frequency was found to increase gradually below 0.4 K. This was then shown to rise at a $T_R$ of 0.33 K. With a further decrease in temperature to 0.2 K, the resonant frequency was then found to decrease. Above 0.10 atom/nm$^2$ $^3$He, a sharp increase in frequency at $T_R$ became apparent. The $^3$He areal density increased with an increase in the $T_R$. No change was observed for the $T_D$.

The inset in Fig. 3 shows a phase diagram, divided into four regions, characterized by decoupling and sticking behaviors. At high temperatures, the $^4$He solid layer tends to stick to the oscillating substrate (stick I). As the temperature decreases, this layer undergoes decoupling below $T_S$ (slip I), where it sticks suddenly at $T_D$ (stick II), regardless of whether the film contains $^3$He. Through the addition of $^3$He, the reentrant mass decoupling appears below $T_R$ (slip II).

When discussing the potential mechanisms of reentrant mass decoupling, it should be noted that both $T_D$ and $T_R$ appear whenever the film overlayer becomes a superfluid. For the pure $^4$He film, sticking at the $T_D$ is caused by the cancellation of mass transport owing to the counterflow of the superfluid overlayer [13].

To further develop this scenario, we can elucidate the reentrant behavior of mass decoupling. A schematic of the $^3$He-$^4$He mixture films is shown in Fig. 4. Because the $^3$He

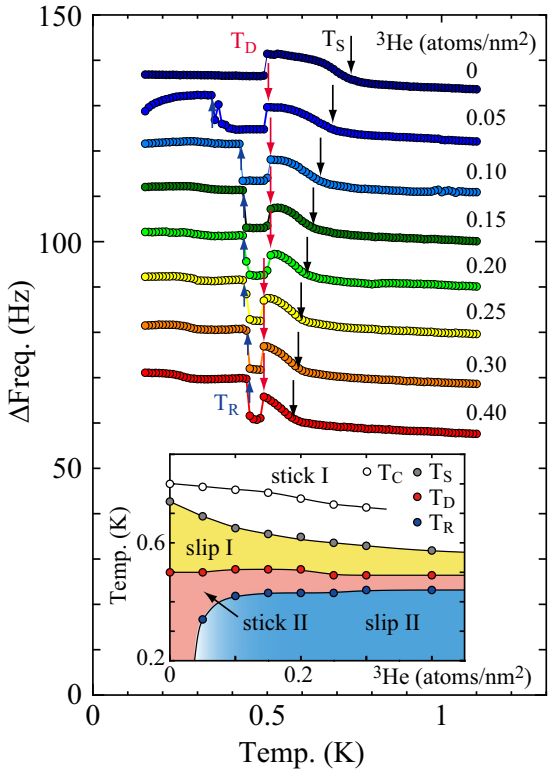


FIG. 3. Variations in the resonant frequency of a 29.3 atoms/nm$^2$ $^4$He film at a 0.25-nm amplitude for various $^3$He areal densities. Arrows indicate the decoupling temperature $T_S$, the sticking temperature $T_D$, and the reentrant decoupling temperature $T_R$. Data are shifted vertically. Inset: Phase diagram of decoupling and sticking behaviors. Here, $T_S$, $T_D$, and $T_R$ are input from Fig. 3, whereas $T_C$ is input from Fig. 1 (run A).

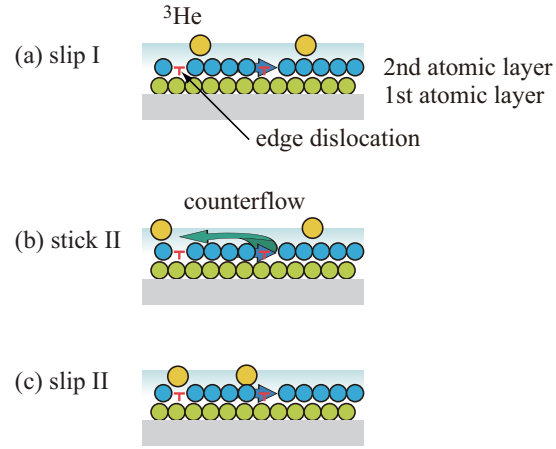


FIG. 4. Schematic of the $^3$He-$^4$He mixture films. The position of the edge dislocation is represented by the ⊤ symbol. (a) Slip I. The second solid layer undergoes decoupling from the first solid layer owing to the motion of edge dislocations. (b) Stick II. When the film overlayer becomes superfluid, $^4$He atoms dissolve in the overlayer at the densified region, while they condense to the second solid layer in the rarefied region. Between the pair regions, the supercurrent transports $^4$He atoms. This process cancels the mass transport owing to the dislocation motion. (c) Slip II. The exchange between liquid and solid $^4$He atoms is prevented by the adsorption of $^3$He atoms.

atoms are spread over the entire fluid overlayer at high temperatures, the $^4$He solid layer can decouple at $T_S$ and then stick at $T_D$, similarly to that of the pure $^4$He film [Figs. 4(a) and 4(b)]. As mentioned previously, sticking at $T_D$ means that the superfluid transport between the edge dislocations cancels the mass transport owing to the dislocation motion. As the temperature decreases, the $^3$He atoms start to adsorb on the edge dislocation at $T_3$, which prevents the exchange between liquid and solid $^4$He atoms [Fig. 4(c)], causing the superfluid transport to cease. The $^4$He solid layer undergoes decoupling at $T_R$.

### B. $^4$He areal density dependence

To determine the dependence of the $^4$He areal density, we conducted temperature sweep experiments for a fixed number of $^3$He atoms through a change in the $^4$He areal density (run B). Figure 5 shows the variation in resonant frequency for several $^4$He areal densities containing 0.20 atom/nm$^2$ $^3$He. The oscillation amplitude was fixed at 0.18 and 0.018 nm during the temperature sweep.

At an amplitude of 0.18 nm, all data points were taken during the warming process. For a $^4$He film of 28.5 atoms/nm$^2$, the resonant frequency was found to increase at a $T_S$ of 0.64 K, which is attributed to the mass decoupling of the $^4$He solid layer. For a $^4$He film of 29.0 atoms/nm$^2$, the mass decoupling was seen to terminate abruptly at a $T_D$ of 0.52 K, whereas a reentrant mass decoupling occurred at a $T_R$ of 0.39 K, which is similar to the behavior shown in Figs. 2 and 3. As the $^4$He areal density increased, the mass decoupling connected to the $T_S$ was found to disappear, whereas that of the $T_R$ remained. With a further increase in the $^4$He areal density, the $T_R$ was found to shift to a lower temperature before disappearing at approximately 39.0 atoms/nm$^2$ $^4$He.

At an amplitude of 0.018 nm, all data points were taken during the cooling process. For a $^4$He film of 28.5 atoms/nm$^2$, it was difficult to determine the $T_3$ accurately. The $T_3$ was, however, observed at 0.40 K for a $^4$He film of 29.0 atoms/nm$^2$. As the $^4$He areal density increased, the $T_3$ was found to shift to lower temperatures. Above a $^4$He film of 35.0 atoms/nm$^2$, the $T_3$ was also difficult to distinguish. However, it should be noted that $T_3$ shares a $^4$He areal density dependence similar to that of $T_R$, although $T_3$ has a limited range. Nonetheless, the onset of superfluidity was also observed for all areal densities measured. As the $^4$He areal density increased, the $T_C$ was found to move to a higher temperature, reaching 1.23 K at a $^4$He film of 39.0 atoms/nm$^2$.

Figure 6 shows the phase diagram of the sticking and decoupling behaviors for a $^3$He areal density of 0.20 atom/nm$^2$. Here, $T_S$, $T_D$, and $T_R$ were obtained from an amplitude of 0.18 nm, whereas the amplitudes at $T_C$ and $T_3$ were measured as 0.018 nm. In contrast to Fig. 3, both regions in sticks I and II and those in slips I and II connect continuously. As previously mentioned, $T_3$ is adjacent to $T_R$. This strongly supports the notion that the adsorption of $^3$He atoms on the edge dislocations causes reentrant mass decoupling.

Moreover, the disappearance of $T_R$ at a high $^4$He areal density may be explained by the competitive adsorption process between the edge dislocation and the free surface. For bulk

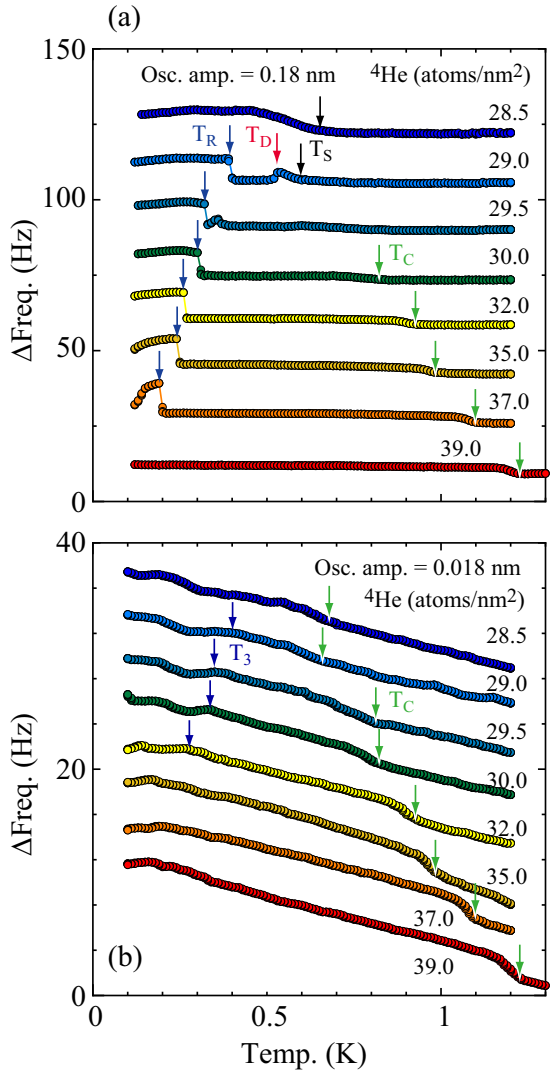


FIG. 5. Variation in resonant frequency at amplitudes of (a) 0.18 nm and (b) 0.018 nm for various $^4$He areal densities containing 0.20 atom/nm$^2$ $^3$He. $T_R$. Data are shifted vertically (run B).

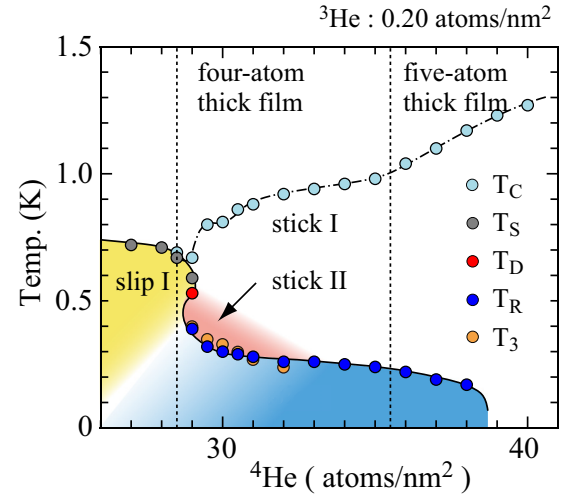


FIG. 6. Phase diagram for the sticking and decoupling behaviors of 0.20 atom/nm$^2$ $^3$He. Here, $T_S$, $T_D$, and $T_R$ were taken at 0.18-nm amplitude. Both $T_C$ and $T_3$ were derived from an amplitude of 0.018 nm.

liquid $^4$He, it is well established that $^3$He atoms are bound to the free surface at low temperatures [17]. The binding energy primarily originates from the difference in the zero-point energy between the bulk liquid $^4$He and that on the free surface. Thus, we propose that, in the case of atomic-thin overlayers, $^3$He atoms would be located on the $^4$He solid layer because of the lack of advantage of zero-point energy on the free surface. When the $^4$He areal density increases, i.e., the overlayer becomes thick, the $^3$He atoms tend to move to the free surface, where the adsorption of $^3$He atoms no longer occurs.

### C. Calculation models for $^3$He adsorption

We discuss the $^3$He areal density dependence on $T_3$ using a simple adsorption model. When building this model, we refer to the previous experiments undertaken on a $^3$He-$^4$He mixture thin film [18,19].

Saunders and coworkers conducted heat capacity experiments on $^3$He above a $^3$He areal density of 0.4 atom/nm$^2$ in $^4$He films of 33.5 atoms/nm$^2$ on Grafoil. They reported that the $^3$He atoms in the $^4$He thin films behave as a two-dimensional (2D) Fermi gas [18]. Hallock and coworkers carried out nuclear magnetic resonance experiments using a 0.1 monolayer of $^3$He in $^4$He thin films on a Nuclepore [19]. They reported that certain parts of the $^3$He atoms are immobile below a critical $^4$He areal density. As the $^4$He areal density increased, the $^3$He atoms were found to experience a mobility edge.

The present observations are similar to those of Hallock and coworkers, in that a small number of $^3$He atoms localized in the $^4$He thin films were found to vanish at a certain $^4$He areal density. Sanders and coworkers concluded that the $^3$He atoms in a $^4$He thin film did not adsorb on Grafoil. We postulate, however, that there is a slight possibility that a small number of $^3$He atoms do adsorb, as the heat capacity is normally independent of the areal density for a 2D Fermi gas.

Because of these considerations, we consider the following model in which the $^3$He overlayer atoms behave as a 2D Fermi gas, leading to the hydrodynamic effective mass $m_3^*$. A surface binding state also exists with an adsorption site density $N_a$ and binding energy $\varepsilon_a$, measured from the 2D Fermi gas. In this model, the adsorption density $n$ is denoted

$$n = N_a \frac{e^{-\beta(-\varepsilon_a-\mu)}}{1+e^{-\beta(-\varepsilon_a-\mu)}} + \frac{2}{(2\pi)^2}\int_0^\infty \frac{2\pi k\, dk}{e^{\beta(\varepsilon-\mu)}+1}, \qquad (2)$$

where $\beta = 1/k_BT$ is the inverse temperature, $\varepsilon = \hbar^2k^2/2m_3^*$ is the kinetic energy of the Fermi gas, and $\mu$ is the chemical potential determined from the $^3$He areal density.

Here, we adopt $m_3^*/m_3$ as 1.5 from the heat capacity experiments for $^4$He films at 33.5 atoms/nm$^2$ [18], although the $m_3^*$ values in thinner $^4$He films are still unknown. The inset in Fig. 7 shows a typical calculation of $n$ as a function of temperature for several $^3$He areal densities with $m_3^*/m_3 = 1.5$, $N_a = 0.06$ sites/nm$^2$, and $\varepsilon_a = 1.268$ K. Here, parameters were chosen where $n = 0.05$ atom/nm$^2$ at 0.43 K for $^3$He

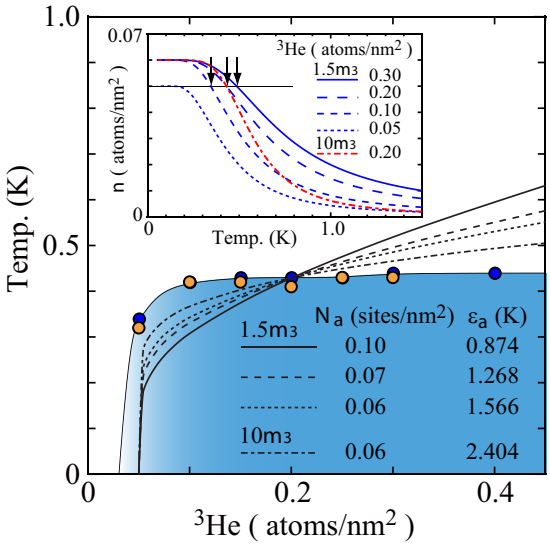


FIG. 7. Comparative graph between the calculation model and $T_3$. Open and filled circles denote $T_3$ in Fig. 1 and $T_R$ in Fig. 3, respectively. The $^4$He areal density was set at 29.3 atoms/nm$^2$. Each line represents the temperature at which $n$ equals 0.05 atom/nm$^2$. For the calculation model, the parameters were chosen as 0.43 K when $n = 0.20$ atom/nm$^2$.

of 0.20 atom/nm$^2$. For comparison, we plotted the curve for $m_3^*/m_3 = 10$ at 0.20 atom/nm$^2$.

As shown in the inset, $n$ increases gradually at high temperatures before becoming almost equal to $N_a$. As the $^3$He areal density increases, $n$ is seen to shift to a higher temperature. Although it is not clear which value of $n$ corresponds to $T_3$, it is assumed that $n_C = 0.05$ atom/nm$^2$ at $T_3$. We plotted the temperature at $n_C$ as a function of the $^3$He areal density in Fig. 7. It was found that the calculated lines have a stronger dependence than the observed ones on the $^3$He areal density. This behavior is independent of the parameters $N_a$, $\varepsilon_a$, and $n_C$. We therefore conclude that this simple model does not fully describe the dependence of $T_3$ on the $^3$He areal density.

As shown in Fig. 7, when we selected $m_3^*/m_3 = 10$, we found $n$ to vary rapidly within a small temperature range, i.e., when the number density just above the surface binding energy is sufficiently large for $T_3$ not to depend strongly on the $^3$He areal density. This suggests that the $^3$He atoms in extremely thin overlayers are almost localized on the Grafoil. It has been reported that $m_3^*$ is enhanced with a decrease in the $^4$He areal density for the Nuclepore [19]. Furthermore, when an attractive interaction between the adsorption sites exists, $n$ is shown to vary more rapidly. Further studies are required to determine this behavior.

For thicker overlayers, $T_3$ could not be determined clearly above a $^4$He film of 33.0 atoms/nm$^3$. However, it is natural to assume that $T_3$ is almost equal to $T_R$, meaning that $T_3$ tends to be 0 at a $^4$He film of approximately 39.0 atoms/nm$^3$. As mentioned in Sec. III B, the $^3$He atoms are bound to the free surface of the bulk liquid $^4$He [17]. Here, the binding energy $\varepsilon_S$ was found to be $2.22 \pm 0.03$ K. This means that $\varepsilon_a$ is smaller than $\varepsilon_S$.

## IV. SUMMARY

In this study, we used a QCM technique with a 5-MHz AT-cut crystal to determine the mass-decoupling behavior of the $^3$He-$^4$He mixture films on Grafoil. In a four-atom-thick $^4$He film of 29.3 atoms/nm$^2$, we observed the following behaviors: (a) For a low, 0.018-nm, amplitude, a slight decrease in resonant frequency occurs at $T_3$. (b) For a high, 0.25-nm, amplitude, mass decoupling at $T_S$ and sticking at $T_D$ were observed to be the same as those for the pure $^4$He films. In addition to $T_S$ and $T_D$, reentrant mass decoupling was found to occur at a $T_R$ adjacent to the $T_3$. Here, it was found that both $T_3$ and $T_R$ are independent of the $^3$He areal density above 0.1 atom/nm$^2$ at ~0.4 K.

From our previous studies on pure $^4$He films, we proposed the following scenario: the mass decoupling below $T_S$ results from the motion of edge dislocations between the first and the second solid layers. The mass sticking at $T_D$ is caused by the cancellation of mass transport owing to the counterflow of the superfluid overlayer [13]. As an extension of this scenario, the observed behaviors can be explained as follows. $^3$He atoms, which are mobile at high temperatures, are localized on edge dislocations at $T_3$. These $^3$He atoms prevent the exchange between liquid and solid $^4$He atoms, and the reentrant mass decoupling occurs after the superfluid counterflow ceases.

By changing the $^4$He areal density to 0.2 atom/nm$^2$ $^3$He, we found that $T_R$ decreases with increasing $^4$He areal density and disappears above a $^4$He film of 29.0 atoms/nm$^2$. This behavior can be explained by competitive adsorption between the edge dislocation and the free surface.

These observations naturally suggest a model that the $^3$He atoms adsorb on the $^4$He solid layer. However, this model does not explain the weak $^3$He areal density dependence on $T_R$ using the hydrodynamic effective mass of $^3$He in the overlayer. Further studies are required to study this behavior.

## ACKNOWLEDGMENTS

T.M. wishes to express his thanks for the financial support received from the Yamaguchi Educational and Scholarship Foundation.

[1] D. S. Greywall and P. A. Busch, Phys. Rev. Lett. **67**, 3535 (1991); D. S. Greywall, Phys. Rev. B **47**, 309 (1993).
[2] P. A. Crowell and J. D. Reppy, Phys. Rev. B **53**, 2701 (1996).
[3] M. Pierce and E. Manousakis, Phys. Rev. B **59**, 3802 (1999).
[4] P. Corboz, M. Boninsegni, L. Pollet, and M. Troyer, Phys. Rev. B **78**, 245414 (2008).
[5] M. Neumann, J. Nye'ki, B. Cowan, and J. Saunders, Science **317**, 1356 (2007).
[6] H. Fukuyama, J. Phys. Soc. Jpn. **77**, 111013 (2008).
[7] J. Nyeki, A. Phillis, A. Ho, D. Lee, P. Coleman, J. Parpia, B. Cowan, and J. Saunders, Nat. Phys. **13**, 455 (2017).
[8] J. Krim, Adv. Phys. **61**, 155 (2012).

[9] A. Dayo, W. Alnasrallah, and J. Krim, Phys. Rev. Lett. **80**, 1690 (1998); M. Highland and J. Krim, *ibid.* **96**, 226107 (2006).
[10] L. Bruschi, A. Carlin, and G. Mistura, Phys. Rev. Lett. **88**, 046105 (2002); A. Carlin, L. Bruschi, M. Ferrari, and G. Mistura, Phys. Rev. B **68**, 045420 (2003).
[11] N. Hosomi, A. Tanabe, M. Suzuki, and M. Hieda, Phys. Rev. B **75**, 064513 (2007).
[12] N. Hosomi and M. Suzuki, Phys. Rev. B **77**, 024501 (2008).
[13] N. Hosomi, J. Taniguchi, M. Suzuki, and T. Minoguchi, Phys. Rev. B **79**, 172503 (2009).
[14] N. Hosomi and M. Suzuki, J. Low Temp. Phys. **148**, 773 (2007).
[15] J. Krim and A. Widom, Phys. Rev. B **38**, 12184 (1988).
[16] F. Souris, A. D. Fefferman, H. J. Maris, V. Dauvois, P. Jean-Baptiste, J. R. Beamish, and S. Balibar, Phys. Rev. B **90**, 180103(R) (2014).
[17] D. O. Edwards and W. F. Saam, *Progress in Low Temperature Physics, Vol. VIIa*, edited by D. F. Brewer (North-Holland, Amsterdam, 1978), pp. 283–369.
[18] M. Dann, J. Nyéki, B. Cowan, and J. Saunders, J. Low Temp. Phys. **110**, 627 (1998).
[19] D. T. Sprague, N. Alikacem, and R. B. Hallock, Phys. Rev. Lett. **74**, 4479 (1995); P. A. Sheldon and R. B. Hallock, *ibid.* **77**, 2973 (1996).